Published paper
Liskiewicz, T. and Fouvry, S. (2005) *Development of a friction energy capacity approach to predict the surface coating endurance under complex oscillating sliding conditions.* Tribology International, 38 (1). pp. 69-79. ISSN 0301-679X
http://dx.doi.org/10.1016/j.triboint.2004.06.002

Development of a friction energy capacity approach to predict the surface coating endurance under complex oscillating sliding conditions

T. Liskiewicz, S. Fouvry*

Laboratoire de Tribologie et Dynamique des Systèmes, CNRS UMR 5513, Ecole Centrale de Lyon, 36 Avenue Guy de Collongue, 69134 Ecully Cedex, France

* Corresponding author: tel.: +33-472-186562; fax: +33-478-433-383.

E-mail address: siegfried.fouvry@ec-lyon.fr (S. Fouvry).

Abstract

In the case of surface coatings application it is crucial to establish when the substrate is reached to prevent from catastrophic consequences. (DELETE : Moreover, a reliable selection of surface treatment is of great interest to industrial applications. However, regarding the lifetime of the coatings, selection criteria often depends on the experimental approaches as well as contact configuration and then can not be directly applied to real cases.)

In this study a model based on local dissipated energy is develop and related to the friction process. Indeed, the friction dissipated energy is a unique parameter that takes into account the major loading variables which are the pressure, sliding distance and the friction coefficient. To illustrate the approach a sphere/plane (Alumina/TiC) contact is studied under gross slip fretting regime. Considering the contact area extension the wear depth evolution can be predicted from the cumulated dissipated energy density. Nevertheless, some difference is observed between the predicted and detected surface coating endurance. This has been explained by a coating spalling phenomenon observed below a critical residual coating thickness. Introducing an effective wear coating parameter the coating endurance is better quantified and finally an effective energy density threshold, associated to a friction energy

capacity approach, is introduced to rationalize the coating endurance prediction. The surface treatment lifetime is then simply deduced from an energy ratio between this specific energy capacity and a mean energy density dissipated per fretting cycle. The stability of this approach has been validated under constant and variable sliding conditions and illustrated through a Energy Density–Coating Endurance chart.

Keywords: coating endurance; TiC; energy wear approach; fretting wear; variable sliding conditions.

1. Introduction

Surface coatings are classically used in industrial applications to reduce friction and wear [1]. The coating is usually selected on a ”trial and error” basis, which is time consuming and expensive. That is why laboratory tests have been developed to quickly preselect coating palliatives. However the absence of fundamental variables and explicit formulations precludes predicting the surface treatments life time. Moreover, the analysis of variable sliding amplitude situations, classically observed in industrial applications, has been greatly discouraged again due to the lack of success of cumulative damage studies. The aim of this work is to show how, by applying an energy approach and its derivation to a local energy density wear formulation, the wear volume evolution and the lifetime of coatings, respectively, can be predicted. This will be done by analyzing a TiC hard coating under oscillating sliding contacts: so-called fretting. Fretting wear is applied in this study due to its wide presence in industrial components.

Fretting is defined as the loading and consequent damage between two surfaces in contact subjected to small tangential displacement (of the order of a few microns) [2,3]. Fretting

occurs in many assemblies where vibrations are likely: suspension cables, dovetail contact in turbine engines, electrical connectors, heat exchangers [4]. The smallest displacement amplitudes are related to partial slip conditions in which the contact displays both, stick and slip domains [5]. This sliding condition particularly favours crack nucleation and possible propagation. The present study concerns larger displacement amplitudes inducing full sliding through the interface. Such a dissipative gross slip condition induces wear mainly by debris formation and ejection [6]. If fretting cracking phenomena have been extensively investigated, the prediction of the wear kinetics is still of great interest. It is essential to establish when the component needs to be replaced or repaired and do so before catastrophic wear occurs. For instance, hard coatings display high, stable, compressive stresses which prevent surface crack nucleation. When the substrate is reached, cracking may initiate. Therefore, wear may indirectly control the cracking kinetics, which supports the idea of a global approach to fretting contact failure.

2. Experiments

2.1 Fretting apparatus

Fretting tests were carried out using an electrodynamic shaker activating a specific fretting rig illustrated in Figure 1. Tests were conducted in a closed chamber where both ambient and relative humidity were controlled. The normal force (P) is kept constant, while the tangential force (Q) and displacement (δ) are recorded. A reciprocating movement with a constant speed was imposed. Thus the fretting loop $Q - \delta$ can be drawn to extract quantitative variables including the dissipated energy (E_d) (i.e. the area of the hysteresis) [7], the sliding amplitude (δ_g), the displacement amplitude (δ_*), and the tangential force amplitude (Q_*). To obtain a

dynamic overview of the fretting test, the fretting cycles are superimposed, resulting in the fretting log. The cumulated dissipated energy is simply defined as the total sum of the fretting cycle area:

$$\Sigma E_d = \sum_{i=1}^{N} E_{di} \quad (1)$$

A mean friction value defined over the whole fretting cycle appears more pertinent to quantify the wear (Fig. 1b). An energy friction coefficient is then introduced:

$$\mu_e = \frac{E_d}{4.P.\delta_g} \quad (2)$$

Thus, the average value over the test duration is defined from:

$$\overline{\mu}_e = \frac{1}{N} \sum_{i=1}^{N} \frac{E_{di}}{4 \cdot \delta_{gi} \cdot P_i} \quad (3)$$

2.2 Materials

A high speed steel VANADIS 23 (1,28 wt.% C; 4,2 wt.% Cr; 5,0 wt.% Mo; 6,4 wt.% W and 3,1 wt.% V) was used as a substrate material.

The studied 1.6 µm thick TiC coating was deposited by a two step indirect method [8]. A polycrystalline alumina ball with a R=12,7mm radius was used as the counter body. The mechanical and surface properties of materials are summarized in Table 1.

2.3 Loading conditions

Fretting tests were carried out under a 100N normal force loading, ±50 and ±100µm displacement amplitudes and test durations from 5000 up to 50000 cycles with constant 5Hz frequency and 50% relative humidity.

To evaluate the wear model's stability, constant and variable amplitude sliding conditions were applied using a fatigue analogy approach. As illustrated in Figure 2, blocks of different displacement amplitudes were superimposed. The test duration, characterized by a total number of cycles (N), was divided into one, two and four blocks of ±50 and ±100 displacement amplitude defining the studied $(50/100)\mu m_{x1}$, $(50/100)\mu m_{x2}$ and $(50/100)\mu m_{x4}$ sequences respectively.

The wear volume of the fretting scars, denoted as (W), was measured using 2D profilometry equipment. For each wear scar profiles along and across the sliding direction were obtained. To determine the total wear volume, a simplified integration was used [9]. The final contact radius r is measured and the contact area (S) deduced from the optical measurements of the fretting wear scar diameter normal to the sliding direction.

3. Prediction of the wear depth kinetics

The first part of this study mainly includes results given in reference [10]. However, to properly conduct the discussion, some essential aspects are here recalled.

3.1 Friction and wear volume analysis

Figure 3 shows that a TiC/alumina fretting contact displays a stable friction behavior with a mean value stabilized around 0.5.

On the other hand, Figure 4 confirms a linear evolution of the wear volume with the cumulated dissipated friction energy [7,11]. The coating wear resistance can then be quantified through the energy wear coefficient α such as :

$$W = \alpha.\Sigma Ed \qquad (4)$$

For the tested TiC coating we deduced $\alpha = 415\ \mu m^3/J$.

The stability of the energy wear coefficient α has been proved under wide rage of applied normal loads [12]. In the studied case, the linear correlation obtained from a large spectrum of loading conditions confirms again the cumulated dissipated energy parameter as a pertinent variable to predict the wear volume extension.

3.2 Local wear damage analysis: Correlation between an energy density parameter and the wear depth evolution.

The coating endurance is classically related to the substrate reaching condition. Hence, compared to a conventional wear volume analysis, wear depth quantification appears more suitable to predict the coating lifetime [10, 12-14]. However, it requires a local analysis. By considering the dissipated energy as the controlling parameter of wear, we assume that the wear depth is related to the cumulated dissipated energy density. Figure 5 illustrates such a correlation considering a Hertzian shear stress field distribution.

However due to the rapid wear of the interface, a mean pressure field distribution appears more representative. The general expression of the energy density dissipated at the contact center during the i^{th} fretting cycle is expressed as :

$$\text{If } r(i) > \delta_g(i) \cdot \text{ then } E_{dh}(i) = 4 \cdot \delta_g(i) \cdot \mu_e(i) \cdot p_m(i) \quad (5)$$

else,

$$E_{dh}(i) = 4 \cdot r(i) \cdot \mu_e(i) \cdot p_m(i)\,, \quad (6)$$

with the mean pressure $p_m(i)$ equal to

$$p_{m(i)} = \frac{P(i)}{S(i)} = \frac{P(i)}{\pi \cdot r(i)^2} \quad (7)$$

where r(i) and S(i) are respectively the wear scar radius and contact area for the "*-i-th*" fretting cycle. The normal force P(i), the sliding amplitude $\delta_{g(i)}$ as well as the friction coefficient $\mu_{e(i)}$ are continuously recorded and can be re-injected into the formulations. A major difficulty is to extrapolate the surface area S(i) evolution.

Assuming the fretting wear cap to be spherical, both the contact surface (S) and the wear volume (W) can be explicated (the relative notations are referred in Figure 6):

$S = 2\pi Rh$ and $W = \frac{1}{3}\pi h^2(3R - h)$ leads to (8)

$$W = \frac{1}{3}\pi \frac{S^2}{(2\pi R)^2} \cdot R \cdot \left(3 - \frac{h}{R}\right) \text{ therefore with } h << R$$

we deduce

$$W = K \cdot S^2 \text{ with } K = \frac{1}{4\pi R} \quad (9)$$

We may then substitute equation (9) into equation (4) to determine the following expression:

$$S = \left(\frac{\alpha}{K}\right)^{1/2} \cdot \Sigma E d^{1/2} \quad (10)$$

Of course the contact area is not equal to zero at the beginning of the test, and the formulation needs to consider the incipient Hertzian area. Therefore for a given sphere/plane configuration the contact surface extension is assumed to verify the following simple expression:

$$S = A \cdot \Sigma E d^{1/2} + B \quad (11)$$

Figure 7 confirms the reliability of this approximation and the corresponding contact constants are found through a least squares fit to be A= 5300 $\mu m^2/J$ and B= 98500μm^2. For the studied TiC hard coating experimental results obtained through the entire fretting test programme are plotted in Figure 7. Nevertheless, it is not necessary to complete more than four fretting tests to properly determine the empirical parameters *A* and *B* in equation (11). By investigations of other hard coatings, it has been observed by the authors that the *A* parameter (related to the curve slope) refers to the particular coating wear kinetics and remains constant

independently of loading conditions, while *B* parameter (related to curve position on *y*-axis) is a function of applied normal load.

Note that the contact surface as a function of test duration has likewise been measured in reference [10]. However, an error in the commercial software used to measure distances on micrographs induced a critical overestimation of the contact radius, generating inconsistent energy density and obsolete energy density wear factors. This technical aspect has been resolved and the present results have been carefully corrected and verified.

One interesting aspect of this simple fretting scar dimensional analysis is that it also permits energy wear parameters to be rapidly identified. Indeed, knowing the sphere radius and assuming that :

$$\alpha \approx K \cdot A^2 \tag{12}$$

the energy wear parameter α can adequately be estimated.

A numerical application gives $\alpha \approx 176\ \mu m^3/J$. This value is significantly smaller than the value given by more precise surface profiles (4). However, the simplicity of this reverse approach may provide a rapid and low cost estimation of energy wear parameters to compare different surface coatings. Further investigations will be conducted to evaluate how the optimization of such an area quantification, widely employed to characterize wear under abrasion tests, could be applied to fretting wear.

By quantifying the surface area evolution as a function of the cumulated dissipated energy, it is now possible to determine the energy density properly. Hence, the energy density dissipated during the i^{th} fretting cycle is represented by:

$$E_{dh}(i) = 4 \cdot \delta_g(i) \cdot \mu_e(i) \cdot \frac{P(i)}{A \cdot \Sigma E_d(i)^{1/2} + B} \text{ with } \Sigma E_d(i) = \sum_{j=1}^{i} \Sigma E_d(j) \tag{13}$$

and successively the cumulated energy density dissipated during the fretting test deduced by :

$$\Sigma E_{dh} = \sum_{i=1}^{N} E_{dh}(i) \tag{14}$$

This formulation at first seems intricate and complex. However, only linear expressions and regular sums are considered which can easily be implemented in any data post treatment. Automatic procedures have been extensively applied to analyze each fretting test and the results are reported in Figure 8. A linear evolution between the wear depth and the calculated cumulated energy density is observed, confirming the stability of the energy approach to quantify the wear process of such a hard coating.

The wear depth extension can be formalized through the following simple linear relationship:

$$h = \beta \cdot \Sigma E_{dh} \quad (15)$$

with, the β- energy wear coefficient defined from the energy wear depth analysis. Note that the local energy wear parameter $\beta = 474\ \mu m^3/J$ obtained is very close to the volumetric variable $\alpha = 415\ \mu m^3/J$. As expected, this good correlation confirms the necessity to integrate the contact area evolution to correctly predict the wear depth increase.

3.3 Prediction of the coating endurance: development of an energy density – coating endurance chart.

The former local wear depth analysis supports the idea that the coating lifetime could be predicted. Hence, for a given coating thickness (t), we can identify the critical dissipated energy density (E_{dhc}) related to the moment when the substrate is reached:

$$E_{dhc} = \frac{t}{\beta} = 3.4\ 10^{-3}\ J/\mu m^2 \quad (16)$$

One fundamental conclusion of this relationship suggests that the coating endurance is simply related to a critical energy density delivered to the tribo-system.

Thus, for a constant energy density per fretting cycles (E_{dh}) we can determine the critical number of cycles to reach the substrate (Nc) :

$$N_C = \frac{E_{dhc}}{E_{dh}} \quad (17)$$

However, whatever the sliding condition (constant or variable), the energy density is never constant. An increase of the contact area and/or a variation of the sliding amplitude promotes an evolution of the energy density (Figure 9) which suggests that an averaged energy density value should be considered:

$$\overline{E}_{dh} = \frac{\Sigma E_{dh}}{N} \quad (18)$$

therefore,

$$N_C = \frac{E_{dhc}}{\overline{E}_{dh}} \quad (19)$$

By inserting this mean value into equation (17), an energy density – coating endurance chart (i.e. $\overline{E}_{dh}$-N curve), equivalent to the S-N fatigue Wöhler's representation [15], can be introduced. The coating endurance is then formalized as a function of the imposed mean energy density.

To experimentally validate such an assumption, substrate reaching conditions must be determined and compared with the model. This is commonly achieved by marking the friction discontinuity resulting from severe substrate/metal interactions. However, due to the diffusion process involved in elaborating the TiC hard coating, no clear friction discontinuity has been observed. Therefore to determine the coating endurance, the critical number of fretting cycles (Nc) was established by numerous interrupted tests where the substrate reaching conditions were confirmed by surface profiles and optical observations. One should note that some spalling of the coating can appear when the coating is almost worn through. It generates large coating debris and influences the system's kinetics (Fig. 11).

As Figure 10 illustrates, this promotes a slightly shorter coating lifetime than predicted by the volumetric wear model.

3.4 Introduction of the "worn effective coating thickness" concept

The experimental lifetime reduction has been confirmed for all the studied loading conditions. Figure 12 shows that the coating endurance distribution (dotted curve), displays a quasi parallel evolution compared to the theoretical curve (bold curve).

This indicates that the coating life time is not only related to the progressive wear mechanisms but is also a function of more severe mechanisms which ultimately drastically reduce the coating lifetime. As previously mentioned, when the substrate is almost reached, spalling phenomena associated to coating decohesions are observed. Based on these observations we can develop the following scenario:

As wear progresses and the coating becomes thinner, the cyclic stresses imposed through the substrate/coating interface are increased [16]. Above a threshold stress value (i.e. below a critical residual coating thickness), a severe decohesion is activated inducing a general failure. According to this hypothesis, damage evolves as progressive wear controlled by the friction energy, followed by a quasi instantaneous decohesion controlled by a critical overstressing of the substrate interface (Figure 13).

This tendency is quantified by plotting the ratio between the experimental endurance and the theoretical one defined from the wear depth progression (N_{Cexp}/N_{Cth}), as a function of the coating endurance N_{Cexp} (Figure 14). A scattered distribution is observed, characterizing the spalling instability. However a constant tendency can be defined and a mean value around 0.8 approximated. This confirms that the decohesion phenomena seems to be activated for a constant residual coating thickness:

$$t_r = t \cdot \left(1 - \frac{N_{Cexp}}{N_{Cth}}\right) \approx 0.3\ \mu m \qquad (20)$$

Hence considering that similar friction and normal loadings have been applied, we can deduce that this critical residual thickness is in fact related to a constant threshold interface stress (Fig.13).

The damage mechanisms on substrate/coating interface are complex and not fully understood. Further experiments and surface coating modelling will be conducted to develop this hypothesis, where different coating parameters like nominal thickness, surface roughness or adhesion forces will be considered. However the present investigation suggest that two damage mechanisms need to be considered to properly predict the coating endurance.

Given that the coating decohesion is closely related to a threshold stress loading associated to a critical residual coating thickness, the coating endurance can be estimated by introducing an effective critical dissipated energy density " E_{dhe} " so that :

$$E_{dhe} = \frac{t_e}{\beta} \qquad \text{with} \qquad t_e = t - t_r \tag{21}$$

With "t_e" , related to the effective coating thickness removed by the progressive wear process before decohesion.

Again a similar Wöhler description is derived and the coating lifetime is finally given by the following simple expression:

$$N_C = \frac{E_{dhe}}{\overline{E}_{dh}} \tag{22}$$

Considering the calculated effective thickness, a numerical application gives $E_{dhe} = 2.7\ 10^{-3}$ J/µm². The corresponding energy density – coating endurance chart (i.e. $\overline{E}_{dh}$ -N curve) (Figure 15) confirms the stability of the approach, outlining the fact that the contribution of each damage process to the coating lifetime reduction could be formalized through an equivalent consumed coating thickness approach, as previously illustrated in Figure 13.

3.5 Cumulative damage law

It is important to point out that the stability of this wear model is linked to the additive property of the energy variable and the associated linear correlation with the wear damage evolution. To illustrate such a cumulative damage principle a parallel could be drawn with the science of fatigue of materials. Hence considering the additive principle of the energy density, a linear damage accumulation, equivalent to the Miner fatigue expression [17] could be derived. The substrate is reached when the following relationship is verified:

$$\sum \frac{N_i}{N_{iC}} = 1 \tag{23}$$

where, N_i – number of cycles under the "ith" energy density level,

N_{iC} – number of cycles to reach the substrate under the "ith" energy density level.

Note that the linearity and the damage cumulation are encapsulated in the energy density average and the cumulated energy parameters. To illustrate this principle an incremental analysis is presently depicted (Figure 16).

Splitting the 25000 cycles of the coating endurance into 7 appropriate intervals, we deduced:

$$\sum_{i=1}^{7} \frac{N_i}{N_{iC}} = \frac{2500}{17000} + \frac{2500}{19000} + \frac{2500}{21000} + \frac{2500}{24000} + \frac{5000}{26000} + \frac{5000}{28500} + \frac{5000}{26500} = 1.058 \tag{24}$$

The value obtained is coherent with the result obtained from globally averaging the energy density (Figure 15) and confirms that such an approach is useful to quantify coating endurance under variable loading conditions.

4. Synthesis and conclusions

In this research work it has been shown that the wear depth increase under reciprocating, and adequately, fretting sliding conditions can be formalized through a friction energy capacity approach. It has been outlined that the wear surface contact area increase must and can be formalized to properly describe the wear depth extension. However, a significant difference between the experimental coating lifetime and the predicted endurance extracted from the wear depth formalization has been observed. This demonstrates that the coating endurance is related to a friction energy controlled progressive wear phenomenon which can be interrupted by a stress controlled instantaneous decohesion of the substrate interface.

As illustrated in Figure 17, two damage processes must be quantified to obtain a reliable prediction of the coating lifetime. When an "effective worn coating thickness" concept is introduced, an effective energy density threshold is derived which allows a stable and reliable prediction of the coating endurance. The coating endurance is then simply related to a friction energy capacity (i.e. effective energy density threshold) whereas the coating lifetime is related to a ratio between this energy and the mean energy density dissipated per sliding cycle. By exploiting the additive property of the energy variable, a wear damage law is defined, so the coating endurance can be rationalized from constant to variable sliding conditions through the introduction of an energy density – coating endurance chart (i.e. $\overline{E}_{dh}$-N curve).

It is interesting to note that by taking into account the different damage processes, we can explain and perhaps quantify the classical gap observed between industrial loading conditions and basic wear and abrasion laboratory tests [18].

Indeed coating endurance is not only related to the intrinsic wear resistance properties of the coating, but is also a function of the strength of its interface with the substrate. These two aspects are presently considered, respectively, by determining an energy wear coefficient and

introducing the effective worn coating thickness. The weaker the interface is, the smaller the effective worn thickness and the shorter the coating life time.

Finally, this global damage description allows us to formalize a classical result concerning the difference between the observed wear increase of a coated system (i.e. here the wear depth) compared to the expected coating response. By introducing an effective energy density threshold, this aspect is resolved or at least explained.

Acknowledgments

The authors wish to thank the MIRA program of the Region Rhone-Alpes for the financial support of this work.

References

[1] Holmberg K, Matthews A. Elsevier Trib. Ser. Vol. 28, Elsevier Science B.V., 1994.

[2] Waterhouse RB. Fretting Fatigue. Elsevier Applied Science, London, 1981.

[3] Vincent L, Berthier Y, Dubourg MC, Godet M. Mechanics and materials in fretting. Wear 1992; 153: 135-148.

[4] Forsyth PJE, in: R.B. Waterhouse (Ed.), Fretting Fatigue, Elsevier Applied Science, London, 1981, 99.

[5] Mindlin RD, Deresiewicz H. Elastic spheres in contact under varying oblique forces. ASME Trans J Appl Mech E 1953; 20: 327-344.

[6] Vingsbo O, Schön J. Gross slip criteria in fretting. Wear 1993; 162-164: 347-356.

[7] Fouvry S, Kapsa Ph, Vincent L. Quantification of fretting damage. Wear 1996; 200: 186-205.

[8] Wendler B. Simultaneous surface and bulk hardening of HSS steels. Surface Coat Techn 1998; 100-101: 276-279.

[9] Fouvry S, Kapsa Ph, Zahouani H, Vincent L. Wear analysis in fretting of hard coatings through a dissipated energy concept. Wear 1997; 203-204: 393-403.

[10] Liskiewicz T, Fouvry S, Wendler B. Impact of variable loading conditions on fretting wear. Surface Coat Techn 2003; 163-164: 465-471.

[11] Mohrbaker H, Blanpain B, Celis JP, Roos JR. The influence of humidity on the fretting behaviour of PVD TiN coatings. Wear 1995; 180: 43-52.

[12] Fouvry S, Liskiewicz T, Kapsa Ph, Hannel S, Sauger E. An energy description of wear mechanisms and its applications to oscillating sliding contacts. Wear 2003; 255: 287-298.

[13] Sauger E, Fouvry S, Ponsonnet L, Kapsa Ph, Martin JM, Vincent L. Tribologically transformed structure in fretting. Wear 2000; 245: 39-52.

[14] Fridrici V, Fouvry S, Kapsa Ph, Perruchaut P. Impact of contact size and geometry on the lifetime of a solid lubricant. Wear 2003; 255: 875-882.

[15] Langlade C, Vannes B, Taillandier M, Pierantoni M. Fretting behavior of low-friction coatings: contribution to industrial selection. Tribology Int 2001; 34: 49-56.

[16] Gupta PK, Walowit JA. Contact stresses between an elastic cylinder and a layered elastic solid. Journal of Lubrification Techn 1974; 79 (2): 250-257.

[17] Miner MA. Experimental verification of cumulative fatigue damage. Automot Avia Ind 1945; 93: 20-24.

[18] Imbeni V, Martini C, Lanzoni E, Poli G, Hutchings IM. Tribological behaviour of multi-layered PVD nitride coatings. Wear 2001; 251: 997-1002.

Table 1: Mechanical and surface properties of the studied materials.

	E (GPa) Young's modulus	ν Poisson ratio	H Hardness	Ra (µm) Surface roughness
Alumina	370	0.27	2300 $Hv_{0.1}$	0.01
HSS	230	0.3	800 Hv	0.2
TiC (1.6 µm)	450	0.2	1250 $Hv_{0.05}$	0.2

FIGURE CAPTIONS

Figure 1: Illustration of the experimental fretting wear approach : (a) schematic drawing of the fretting rig, (b) analysis of the fretting cycle.

Figure 2: Illustration of the 'block' sliding amplitude approach (TiC/alumina, RH=50%, f=5Hz, P=100N): (a) definition of constant and variable sliding amplitude conditions; (b): associated fretting logs.

Figure 3: Evolution of the TiC / alumina mean friction coefficient versus the applied fretting cycles (TiC/alumina, RH=50%, f=5Hz, P=100N, displacement amplitudes: ■ 50µm, □ 100µm, ♦ (50/100)μm_{x1}, ○ (50/100)μm_{x2} , ● (50/100)μm_{x4}).

Figure 4: Evolution of the TiC wear volume versus the cumulated dissipated energy (TiC/alumina, RH=50%, f=5Hz, P=100N, displacement amplitudes: ■ 50µm, □ 100µm, ♦ (50/100)μm_{x1}, ○ (50/100)μm_{x2} , ● (50/100)μm_{x4}).

Figure 5: Illustration of the energy density approach to quantify the wear depth evolution: application to a Hertzian sphere/plane distribution (a: Hertzian contact radius; q_0 : Maximum Hertzian shear).

Figure 6: Illustration of the spherical cap shape hypothesis of the fretting wear scar.

Figure 7: Evolution of the surface contact area as a function of the cumulated dissipated energy (TiC/alumina, RH=50%, f=5Hz, P=100N); displacement amplitudes: ■ 50µm, □ 100µm, ♦ (50/100)μm_{x1}, ○ (50/100)μm_{x2} , ● (50/100)μm_{x4} , experiments defined from optical measurements; —— theoretical evolution defined from Eq.11 with A=5300μm^2/J and B=98500μm^2.

Figure 8: Distribution of the wear depth versus the cumulated dissipated energy density, identification of the energy density wear coefficient $\beta = 474 \mu m^3/J$, $R^2 = 0.91$; displacement amplitudes: ■ 50µm, □ 100µm, ♦ (50/100)μm_{x1}, ○ (50/100)μm_{x2}, ● (50/100)μm_{x4}, (TiC/alumina, RH=50%, f=5Hz, P=100N).

Figure 9: Evolution of energy density as a function of the test duration (TiC/alumina, δ = 100 µm, RH=50%, f=5Hz, P=100N), identification of the substrate reaching condition (Nc = 24500 cycles).

Figure 10: Introduction of the energy density coating endurance chart: —— Theoretical coating life time based on the energy wear depth prediction (TiC/alumina, $E_{dhc} = 3.4\,10^{-3}\ J/\mu m^2$); □ : experimental identification of the substrate reaching condition (TiC/alumina, δ = 100 µm, RH=50%, f=5Hz, P=100N).

Figure 11: Observation of incipient spalling damage just before the complete destruction of the coating interface (TiC/alumina, RH=50%, f=5Hz, P=100N, δ=(50/100)μm_{x1}, N=29500cycles).

Figure 12: Comparison between experiments and theoretical prediction of the coating endurance: Δ 200µm, ▲(150/200)μm_{x1}, ◊ 150µm, ■ 50µm, □ 100µm, ♦ (50/100)μm_{x1}, ○ (50/100)μm_{x2}, ● (50/100)μm_{x4}, (TiC/alumina, RH=50%, f=5Hz, P=100N); —— Theoretical curve defined from the energy wear depth analysis (Equ.16 , E_{dhc}= 3.4 10^{-3} J/µm²).

Figure 13: Illustration of the coating damage scenario involving first a progressive wear mechanism followed by an instantaneous decohesion of the coating.

Figure 14: Evolution of the ratio between the experimental coating lifetime and the predicted endurance extracted from the wear depth modeling.

Figure 15: Prediction of the coating endurance, taking into account the lifetime reduction due to spalling; displacement amplitudes: Δ 200µm, ▲(150/200)μm_{x1}, ◊ 150µm, ■ 50µm, □ 100µm, ♦ (50/100)μm_{x1}, ○ (50/100)μm_{x2}, ● (50/100)μm_{x4}; (TiC/alumina, RH=50%, f=5Hz, P=100N); —— Practical curve defined from effective coating thickness approach (Equ. 22 , E_{dhe}= 2.7 10^{-3} J/µm²).

Figure 16: Illustration of linear cumulative wear damage approach associated to the energy density concept (Miner's Fatigue analogy) (TiC/alumina, δ = 100µm, RH=50%, f=5Hz, P=100N): (a) : Block segmentation of the energy density evolution (7 intervals), (b) : Prediction of the coating endurance based on the energy density description (Equ. 22 , E_{dhe}= 2.7 10^{-3} J/µm²).

Figure 17: Diagram of the friction energy capacity approach to predict coating endurance. The model integrates both the intrinsic wear resistance of the coating (i.e. wear depth kinetics) and the substrate/coating interface strength (i.e. identification of the residual coating thickness).

Figure 18: Illustration of generalized coating endurance approach: (a) classical description related to specific loading conditions which expresses the wear increase as a function of the loading duration. A gap is observed between the expected coated wear kinetics and the observed response. Indeed, only part of the nominal thickness (t) is consumed by the wear process. Below a critical residual thickness (t_r), a severe decohesion mechanism is activated. This phenomenon is formalized and quantified for any sliding conditions through the introduction of an energy density coating endurance chart (i.e. $\overline{E}_{dh}$-N curve) (b). The coating endurance is associated to a specific energy density and the corresponding lifetime deduced from a energy ratio: $N_c = E_{dh*} / \overline{E}_{dh}$. It has been shown that, considering an effective worn coating thickness (t_e), and deducing an effective threshold energy density (E_{dhe}), the coating endurance is well predicted and both energy-controlled progressive wear and the stress-controlled instantaneous spalling phenomenon are formalized. Finally the gap in terms of coating endurance is well formalized through the residual consumed coating description: $N_r = E_{dhr} / \overline{E}_{dh} = (t_r / \beta) / \overline{E}_{dh}$ (β: energy wear coefficient).

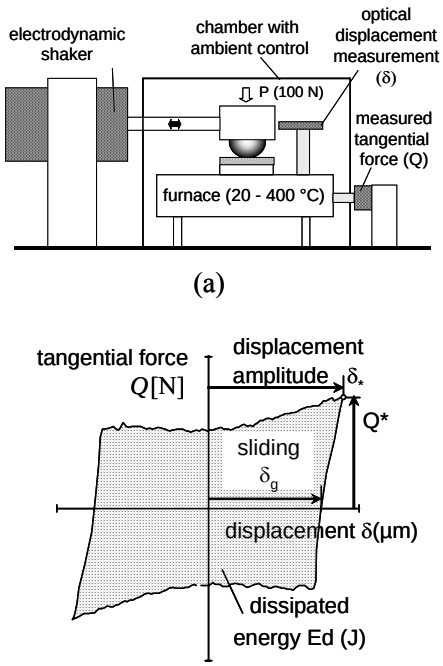
electrodynamic shaker
chamber with ambient control
optical displacement measurement (δ)
P (100 N)
measured tangential force (Q)
furnace (20 - 400 °C)
(a)
tangential force Q[N]
displacement amplitude δ*
Q*
sliding δg
displacement δ(µm)
dissipated energy Ed (J)
(b)

Figure 1

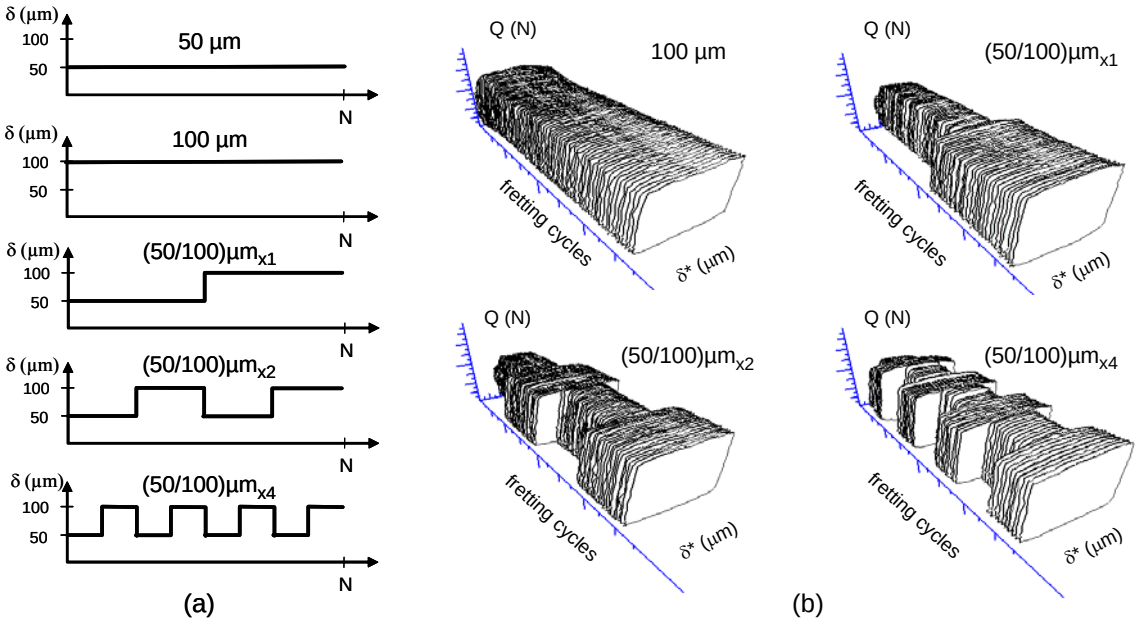

Figure 2

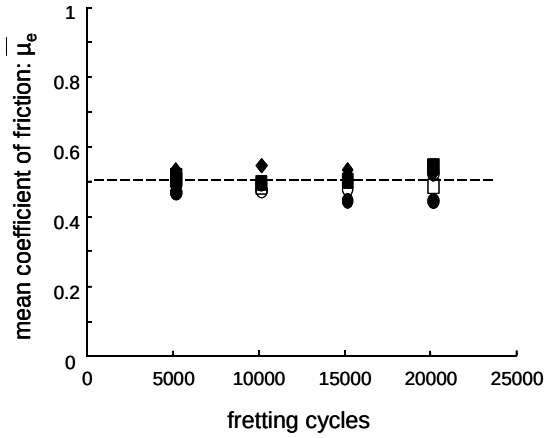

Figure 3

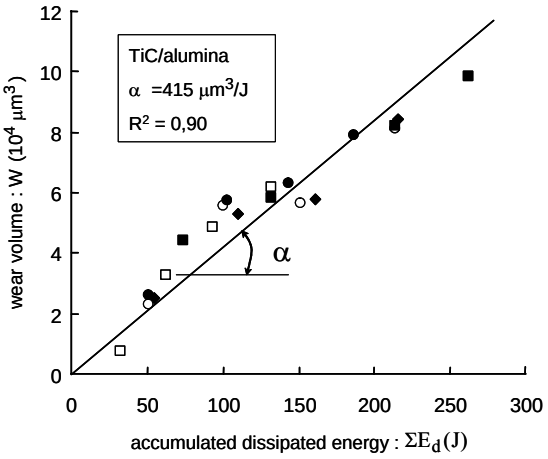

Figure 4

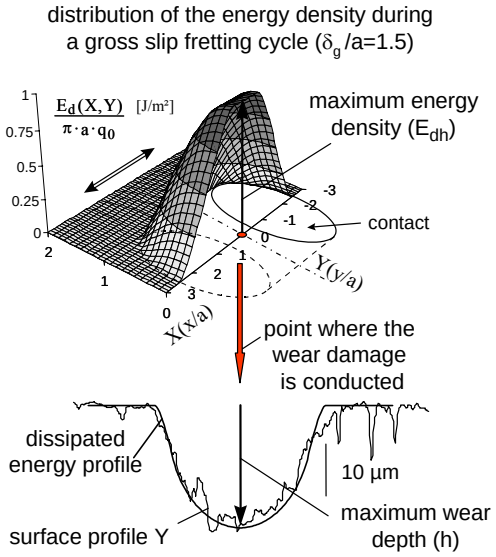

Figure 5

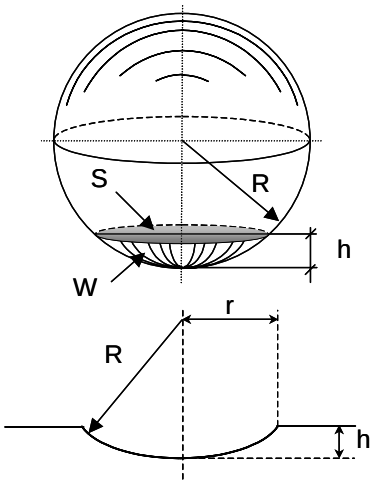

Figure 6

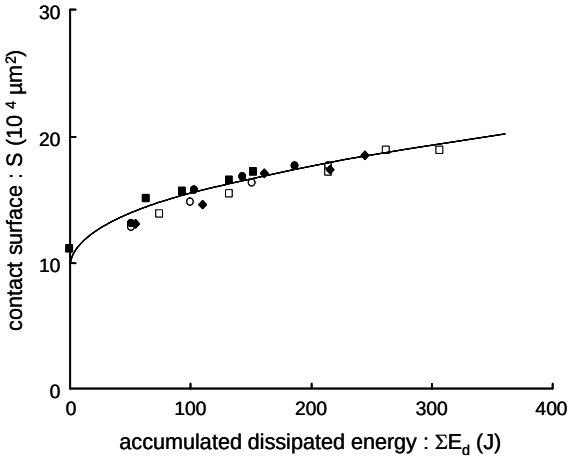

Figure 7

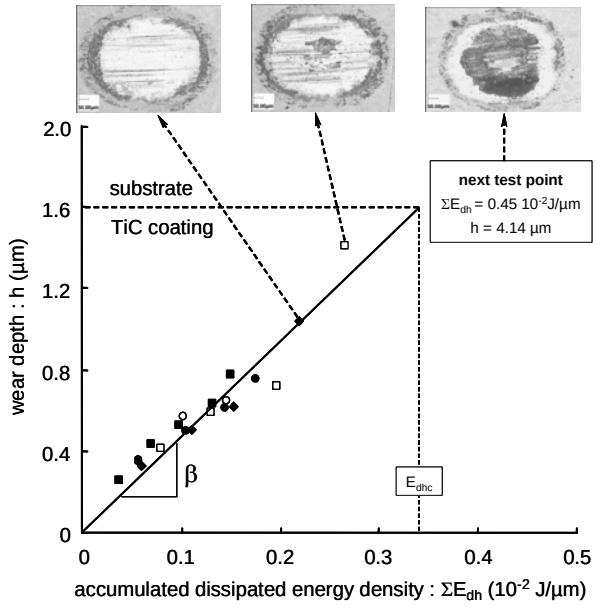

Figure 8

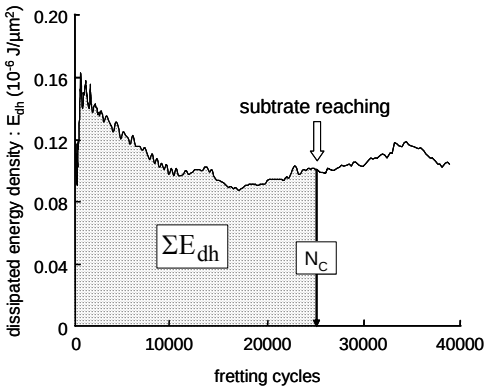

Figure 9

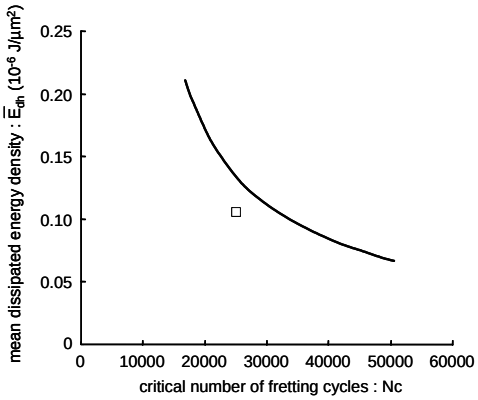

Figure 10

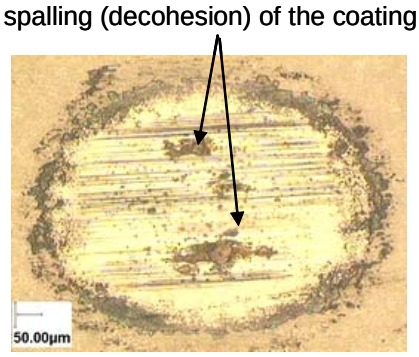

Figure 11

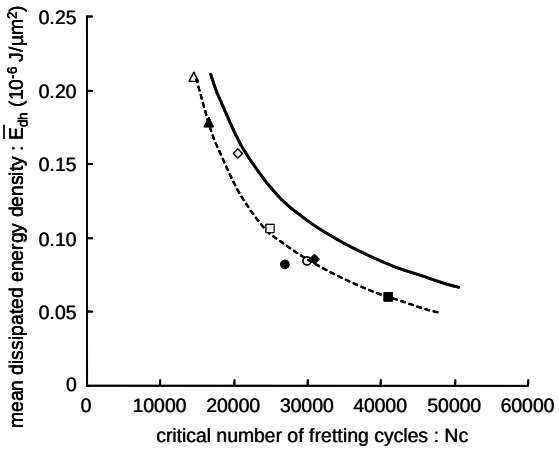

Figure 12

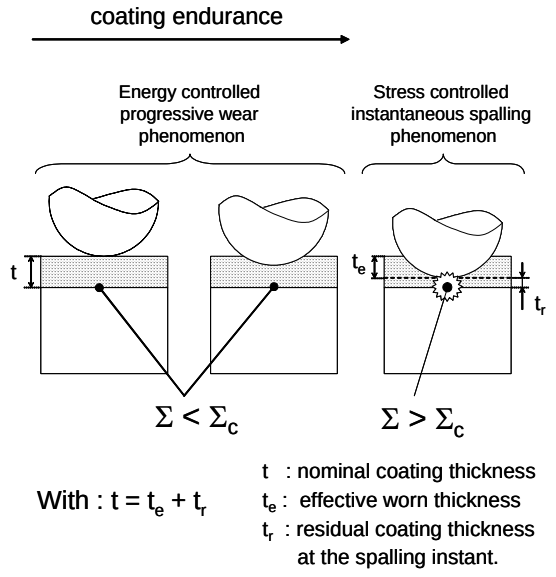

Figure 13

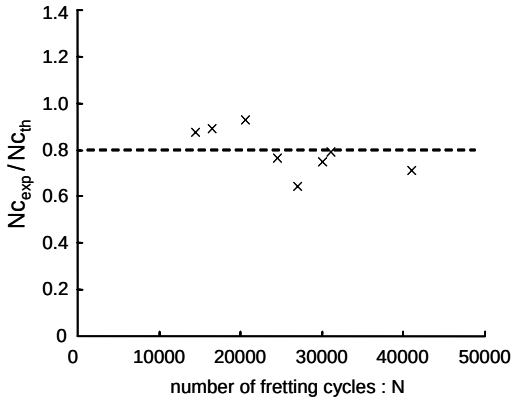

Figure 14

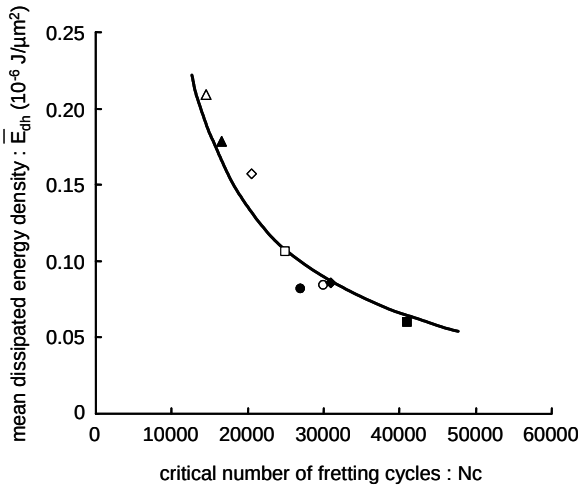

Figure 15

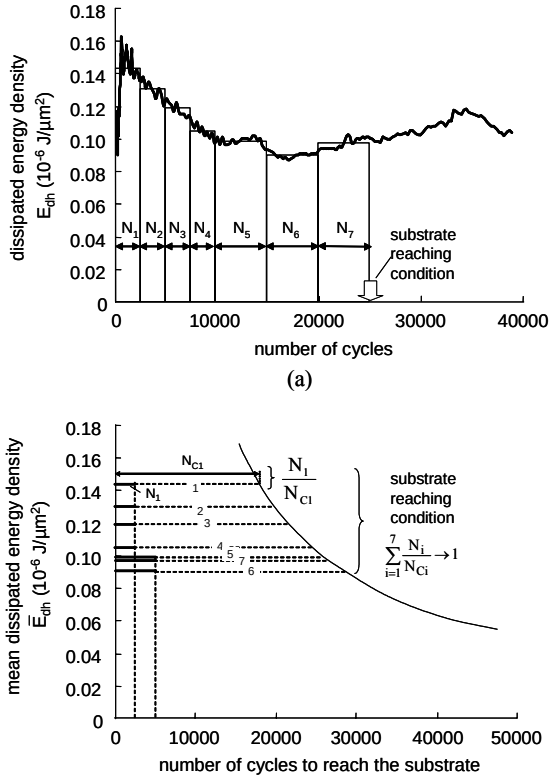
dissipated energy density
E_{dh} (10^{-6} J/μm^2)
0.18
0.16
0.14
0.12
0.10
0.08
0.06
0.04
0.02
0
N_1 N_2 N_3 N_4 N_5 N_6 N_7
substrate
reaching
condition
0
10000
20000
30000
40000
number of cycles
(a)
mean dissipated energy density
$\bar{E}_{dh}$ (10^{-6} J/μm^2)
N_{C1}
N_1
1
2
3
4
5
7
6
$\frac{N_1}{N_{C1}}$
substrate
reaching
condition
$\sum_{i=1}^{7} \frac{N_i}{N_{Ci}} \rightarrow 1$
0
10000
20000
30000
40000
50000
number of cycles to reach the substrate
(b)

Figure 16

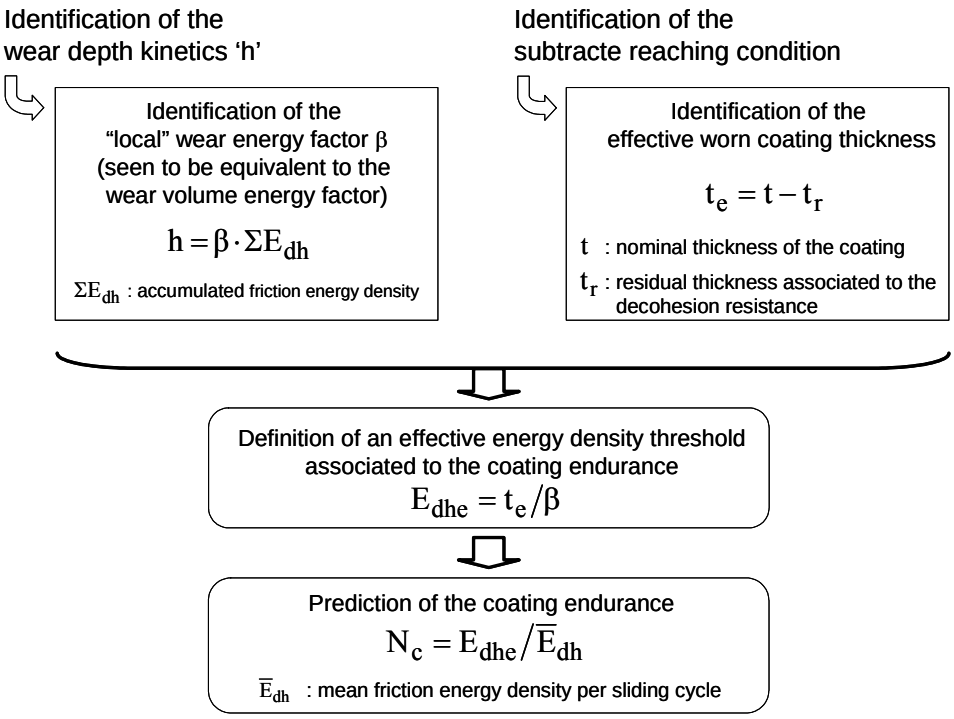
Identification of the
wear depth kinetics 'h'
Identification of the
"local" wear energy factor β
(seen to be equivalent to the
wear volume energy factor)
$h = \beta \cdot \Sigma E_{dh}$
ΣE_{dh} : accumulated friction energy density
Identification of the
subtracte reaching condition
Identification of the
effective worn coating thickness
$t_e = t - t_r$
t : nominal thickness of the coating
t_r : residual thickness associated to the decohesion resistance
Definition of an effective energy density threshold
associated to the coating endurance
$E_{dhe} = t_e / \beta$
Prediction of the coating endurance
$N_c = E_{dhe} / \overline{E}_{dh}$
$\overline{E}_{dh}$: mean friction energy density per sliding cycle

Figure 17

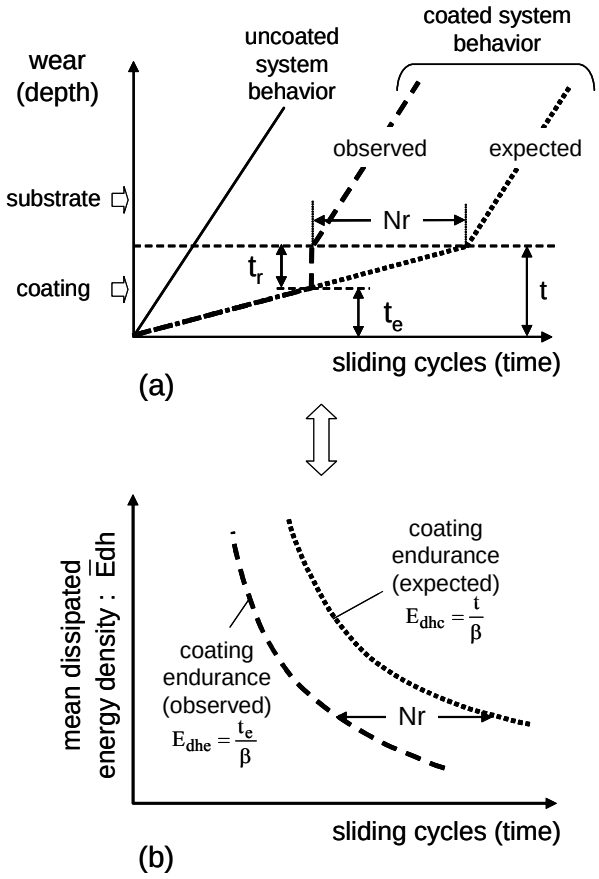
wear
(depth)
uncoated
system
behavior
coated system
behavior
observed
expected
substrate
Nr
coating
t_r
t_e
t
sliding cycles (time)
(a)
mean dissipated
energy density : Edh
coating
endurance
(expected)
$E_{dhc} = \frac{t}{\beta}$
coating
endurance
(observed)
$E_{dhe} = \frac{t_e}{\beta}$
Nr
sliding cycles (time)
(b)

Figure 18